2022-09-07

Exposure of Escherichia coli to cadmium telluride quantum dots, silver nanoparticles or cupric oxide nanoparticles during aerobic respiratory versus anaerobic fermentative growth on <scp>d</scp>-(+)-glucose

Vassallo, J

10.1039/d2en00403h
Environmental Science: Nano
Royal Society of Chemistry

Exposure of *Escherichia coli* to cadmium telluride quantum dots, silver or cupric oxide nanoparticles during aerobic respiratory *versus* anaerobic fermentative growth on D-(+)-glucose

*Joanne Vassallo, Rich Boden and Richard D. Handy**

School of Biological and Marine Sciences, Faculty of Science and Engineering, University of Plymouth, Drake Circus, Plymouth PL4 8AA, UK

*Corresponding author, email: R.Handy@plymouth.ac.uk

Keywords: facultative microbes, antimicrobial, nanomaterials, tellurium, fermentation

Abstract

The antimicrobial effects of engineered nanomaterials (ENMs) on the *Bacteria* are poorly understood in anoxic conditions. Knowing about these effects can better inform environmental risk assessments. This study investigates the inhibitory effects on growth of silver nanoparticles at 3 – 6 mg l^{-1}, CuO nanoparticles at 100 mg l^{-1} or CdTe quantum dots at 3 mg l^{-1} towards *Escherichia coli* K-12 MG1655. These exposure concentrations reflect sub-lethal thresholds identified from a screening exposure in 96-well plates. Uncoated or functionalised ENM variants (negative carboxylate, positive ammonium and neutral polyethylene glycol) are investigated, along with bulk materials or metal salts. Bacterial growth is satisfactory, with test reproducibility of 11 % coefficient of variation in oxic flasks, and 13 % in anoxic serum bottles. Irrespective of the aeration conditions, Ag test materials cause most bacterial growth inhibition, as followed by CdTe and CuO test materials. The bulk form of Ag, CuO and CdTe, as well as the Cu, Cd and Te metal salt cause more growth inhibition under anoxic conditions, compared to oxic conditions (*t*-test, $p < 0.05$). However, by surface coating type, there is no clear trend in bacterial growth inhibition, and this also applies across all test materials. Under anoxia, the appearance of millimolar concentrations of fermentation products confirm that the organism can ferment glucose in the presence of ENMs, but with detrimental effects, as there is less energy available to biologically control the presence of metals. Hence overall, the ENMs are more toxic to *E. coli* in anoxic conditions, suggesting that regulatory tests with microbes that use oxic conditions may underestimate the hazards.

1. Introduction

There is immense bacterial diversity and specialisation within microbial communities in the natural environment, where bacteria are capable of aerobic respiration and/or anaerobic fermentation, with facultative anaerobes often preferring to use oxygen when it is available. Bacteria can be found in many ecological niches in seawater, freshwater, sediments and soils, where the oxygen concentration may also vary.[1] Indeed, microbes such as ‘‘*Cyanobacteria*’’ may generate oxygen during oxygenic photosynthesis in surface water.[2] In contrast, deep down on the seafloor anoxic conditions tend to prevail in sediments; these layers support significant methane production, nitrate and sulfate respiration where heterotrophic bacteria thrive.[3] In soils during flooding events, oxygen can become limited, and bacterial communities adapt from aerobic functioning, to facultative, and to even completely anaerobic growth.[4]

The manufacturing, use, recycling and end-of-life disposal of engineered nanomaterials (ENMs), inevitably contribute to their releases to the environment. Modelling shows that soils

are a major sink for ENMs, predominantly through the application of sewage sludge to soils.[5] For example, the predicted environmental concentrations (PECs) for Ag nanoparticles (NPs) in agricultural soils was around 30 pg kg^{-1} in 2017 and is predicted to reach 10 µg kg^{-1} by 2050; and with PECs that are 30 – 40 higher in sludge-treated soils.[6] Soils are inherently complex ecosystems and in sludge-amended soils naturally occurring microbes will be exposed to aged ENMs.[7] Recent advancements in analytical chemistry allow for direct measurements of some metallic ENMs in environmental matrices including soil,[8] but the effects on ENMs on naturally occurring microbes is only just being understood.

Most microbial ecotoxicological studies published to date have been designed to simulate aerobic growth in the presence of potential bactericidal ENMs, e.g., ZnO, CuO, Ag.[9] Clinical studies have mostly explored ENM toxicity towards facultative microbes, such as the oral pathogen *Strepococcus mutans*[10] and wound-infecting *Staphyloccus aureus* subsp. *aureus*.[11] However, there is also a need to understand how microbes function in naturally low oxygen conditions. Only a few studies have explored bacterial growth in both oxic and anoxic conditions with ENMs. Fortner, et al.[12] exposed two bacterial species, *Escherichia coli* DH5α and *Bacillus subtilis* CB315, to a fullerene C_{60} concentration greater than 0.4 mg l^{-1}; and no bacterial growth was observed in either oxic or anoxic conditions. Taylor, et al.[13] cultured different strains of *E. coli* and *Salmonella enterica* py. Typhimurium in the presence of multi-walled carbon nanotubes (MWCNTs) and toxicity was observed when grown aerobically, and in contrast to growth in anoxic conditions, suggesting that the latter conditions were less hazardous to the microbes. However, the response may also depend on the redox chemistry of the ENM. Zou, et al.[14] found that microbial biodiversity in the presence of Ag NPs varied between surface waters in oxic and anoxic conditions, and might partly arise from the complexation of Ag(I) with sulfide in the latter.

Studies have also explored methanogenic bacteria in wastewater treatment plants exposed to ENMs. Microbes are used to stabilise the sludge and to generate energy mainly through methane production. Nano-forms of CuO, ZnO and CeO_2 caused a dose-dependent decrease in bacterial activity during anaerobic digestion of sewage sludge; whereas no adverse effects were observed following exposure to TiO_2 NPs and inconsistent results were seen with Ag NPs.[15] This suggests that toxicity is material-specific in anoxic conditions. The toxic mechanisms are mostly unknown in anoxic conditions. However, Cu NPs were found to be toxic to methanogens by inhibiting glucose fermentation at 2.5 mg l^{-1} Cu; and with complete inhibition of bacterial fermentation at 40 mg l^{-1} Cu.[16]

Anaerobic growth studies with facultative bacterial models in the presence of ENMs are scarce (e.g., Ag NPs[17-19], Fe NPs[20] and CeO_2 NPs[21]). *E. coli* is widely found in soil and is a good model for environmental studies.[22] Unsurprisingly, it is also abundantly found in sewage sludge.[23] This bacterium grows under oxic and anoxic conditions. In the presence of oxygen it grows by aerobic respiration, whereas in sufficiently low oxygen concentrations an alternative electron acceptor to oxygen, e.g., the nitrate ion, is used.[24] In the complete absence of an electron acceptor *E. coli* is able to grow *via* mixed-acid fermentation.[25] Clearly, understanding the microbial toxicity of ENMs in both oxic and anoxic conditions will enable more accurate environmental risk assessments, as well as clarifying the applicability of standardised microbial degradation tests used in hazard assessment for ENMs (e.g., OECD test guidelines 301-304[26]).

The present investigation primarily sought to assess the antibacterial potential of Ag NPs, CuO NPs and CdTe QDs towards *E. coli* K-12 MG1655 grown under anoxic conditions in sealed serum bottles. Copper is an essential biological element, whereas silver, cadmium and tellurium are not.[27] A secondary aim was to evaluate any differences in the bacterial response to the presence of uncoated or coated (functionalised) ENM variants, specifically as described in Table 1: carboxylic acid (-COOH), ammonium ($-NH_4^+$) and polyethylene glycol-coated types, representing a negative, positive and neutral surface functionalisation, respectively. Microscale (bulk) material counterparts or metal salts, as appropriate, were also tested. The study also aimed to measure the concentration of bacterial fermentation products in the presence of the different test materials, under anoxic conditions, as a result of mixed-acid fermentation; namely the concentrations of acetate, ethanol, formate, and D-, L-lactate. This work also explored any differences in the observed bacterial growth responses in sealed serum bottles, as compared to aerobic bacterial growth in well-aerated Erlenmeyer flasks.

2. Methods

2.1 Bacterial Culture

All glassware was cleaned and deionised by washing overnight with 5 % (*v/v*) nitric acid (Fisher, Primar Plus) and then dried in a hot-air oven. *E. coli* K-12 MG1655 (DSM 18039) (Migula 1895) Castellani and Chalmers 1919 was initially stored in glycerol as a cryoprotectant. This derivative of the K-12 strain was chosen as it has been cured of plasmids, virulence factors and phages; thus it gives more consistent behaviour *in vitro* and also has a high specific growth rate. A batch culture of *E. coli* K-12 MG1655, prepared to ensure a consistent inoculum supply,[22] was grown for 12 h at 37 ºC with shaking at 130 rpm (New Brunswick Scientific Model G25),

then harvested by centrifugation (Harrier 18/80R) at 4 °C, 10,000 × *g* for 30 min, washed and suspended in sterile saline (0.90 % (*w/v*) NaCl, 155 mM). The culture was then diluted to a final optical density (*OD*) at 440 nm *circa* 0.90 (Jenway 7315 UV/Visible Spectrophotometer) and stored at - 80 °C until required for the experiments.

Concentrations of dry biomass (mg l^{-1}) were determined using optical density at 440 nm *versus* calibration curves; an OD_{440} of 0.1 corresponding to 14 mg dry biomass l^{-1}.[22] E-basal salts (EBS) was used as a minimal defined growth medium (*viz*. pH 7.2, 0.314 M ionic strength) and supplemented with 10 mM D-(+)-glucose (Sigma, ≥ 99.5 % purity) as the sole carbon and energy source.[22] Growth curve analysis of *E. coli* K-12 MG1655 was carried out separately in oxic 250 ml Erlenmeyer flasks and in anoxic 120 ml sealed glass serum bottles (Fig. S2). To sterile flasks (n = 3) stoppered with a foam bung, 45 ml of sterile EBS were added, followed by 10 % (*v/v*) inoculum. Similarly, in sterile serum bottles (n = 3) the inoculum addition was followed by the EBS to the brim, until a positive meniscus was visible. The bottles were then sealed with sterile butyl rubber vaccine stoppers ensuring no trapped air, before crimping into place with aluminium crimp seals. All flasks and serum bottles were incubated at 37 ºC and 130 rpm as before. At hourly intervals, 1 ml was sampled from each flask or bottle and turbidity was measured at OD_{440} (Jenway 7315 UV/Visible Spectrophotometer). A sterile hypodermic needle attached to a syringe was used each time 1 ml of culture was extracted from the serum bottles. The volume of air was each time replaced with N_2 gas in order to maintain anoxia without a fall in pressure.

Elemental microanalyses were carried out on bacterial cell suspensions grown aerobically and anaerobically, respectively (Fig. S3). The cell suspensions were harvested by centrifugation (Harrier 18/80R) for 15 minutes at 4500 × *g*, with cooling at 4 ºC and rinsed twice with ice-cold distilled water (double-quartz distilled water, 18 MΩ resistance; used within 10 days of distillation in order to avoid significant uptake of CO_2 from the air). The resulting pellets were dried to constant mass (Gallenkamp OV-160) at 85 ºC in glass beakers, loosely covered with foil. Dried bacterial samples (n = 3), from both aerobic and anaerobic *E.coli* K-12 MG1655 grown cultures, were sent for carbon, hydrogen, oxygen, nitrogen, and sulfur (CHONS) analysis (Elemental Microanalysis Ltd, UK), with carbon, hydrogen, nitrogen and sulfur analysed by the Dumas[28] combustion method and oxygen by the Unterzaucher[29] pyrolysis method. Each biological replicate was analysed as two technical replicates.

158 **2.2 Test Suspensions Preparation and Characterisation of Nanomaterials**

159 The characterisation details of the test materials investigated in this study, including
160 composition, primary particle size, purity, surface area, zeta potential, and total metal
161 concentration measurements in oxic and anoxic conditions, have been described in Table 1 and
162 Fig. S4. Details of the behaviour of the nanomaterials and their bulk controls in sterile saline
163 prior to microbial exposure, including mean aggregate size, mean particle concentration and
164 metal dissolution rate, have been presented elsewhere.[22] Ultrasound (sonication) methods were
165 not used in order to avoid potential damage to the surface coatings on the ENMs; instead all
166 test suspensions or solutions were stirred for 3 h (IKA-WERKE R015), set at speed 3. Then, a
167 1:10 dilution of the stock in sterile physiological saline (0.90 % NaCl) was prepared to achieve
168 a working nominal concentration of 100 mg l^{-1}, followed by dilutions in the same to the required
169 nominal concentrations. Physiological saline was used to prevent osmotic stress to the test
170 organism during the exposures, while enabling a suitable dilution for the experiments.

171 The final nominal test concentrations adopted in this study were chosen to reflect sub-
172 lethal thresholds previously identified from the minimum inhibition concentration assay,[22] in
173 order to achieve a comparable exposure between oxic and anoxic conditions. All exposures, in
174 the presence of ENMs, bulk and metal salts equivalent, as appropriate, were assessed at the
175 same tested nominal concentrations. Given that different metals have different toxicities, in
176 order to achieve an equivalent sublethal dose across all substances, it was necessary to utilise
177 different metal concentrations. With silver a higher nominal concentration was adopted during
178 anaerobic growth because Ag is not known to be particularly harmful under anoxic conditions[17].
179 For metal salts, the amount of powder weighed was adjusted to account for the relative mass
180 contribution of the metal species in the uncoated ENMs and bulk controls. The test materials
181 were uncoated and coated (functionalised) ENM variants as follow: carboxylic acid (-COOH),
182 ammonium (-NH_4^+), or polyethylene glycol (-PEG), along the equivalent metal salts or bulk
183 controls (see Table 1 for details). The precise details of how the coatings were synthesised and
184 attached to the ENM core is commercially sensitive information of the suppliers, but for clarity
185 we use the term '–NH_4^+' to mean a primary amino group that has been protonated to form a
186 positively charged state.[22]

187

188 **2.3 Bacterial Exposure Tests**

189 In this study, the term 'test suspension' refers to the dispersion of ENMs or micron scale
190 particles in a liquid, whereas the phrase 'test solution' refers to metal salts or other soluble
191 substance in solution. During the actual exposures, test suspensions/solutions in sterile saline

were diluted with the growth medium and the inoculum; with the resultant exposure medium referred to hereafter as 'NaCl-EBS medium'. Experiments in the 250 ml sterile Erlenmeyer flasks (n = 3) consisted of 41.0 ml of test suspension/solution, with added 4.1 ml EBS supplemented with glucose at 10 mM concentration (sterilised just before plating, 0.2 µm pore-size Minisart Plus filter) and 4.9 ml cell suspension. Flasks were covered with sterile foam bungs to minimise moisture loss during the incubation period. Likewise, the exposures in sterile 120 ml volume capacity serum bottles (n = 3) consisted of 98.0 ml of each test suspension/solution, with 10.0 ml of the EBS with glucose and 12.0 ml inoculum from the batch preparation. The bottles were sealed by means of sterile rubber stoppers.

Abiotic controls were also tested in parallel to account for the turbidity effect of the saline solution and for the turbidity caused by the test suspension or solution (n = 3). A set of normal growth controls for growth in the absence of any test suspensions and positive controls ($HgCl_2$) for complete growth inhibition were also included (n = 3). The flasks and serum bottles were incubated together for 12 h at 37 ºC with shaking at 130 rpm (New Brunswick Scientific Model G25). After the exposure period, each bottle was vigorously shaken by hand for about 30 s to re-suspend any material which may have deposited to the bottom. Then 1 ml aliquots were pipetted from each flask/bottle into cuvettes (Fisher, polystyrene 10 mm path length) and the optical density (OD_{440}) was immediately measured.

The concentration of unconsumed glucose in the test vessels was measured using the Glucose (GO) Assay Kit from Sigma. Briefly, 4 µl of the supernate from the cultures (n = 3 for bacterial growth in flasks and serum bottles) was diluted with 36 µl of distilled water in new flat bottom 96-well plates. Then 80 µl of the reagent mixture were added to each plate well. The microplates were incubated for 30 min at 37 ºC. The reaction was stopped by the addition of 80 µl of 6 M sulfuric acid (Sigma ACS reagent, 95.0 – 98.0 %). Absorbance was determined at 540 nm using the plate reader (VersaMax microplate reader with SoftMax Pro 4.0 software, Molecular Devices, Sunnyvale, CA, USA). The amount of glucose in the wells was calculated using a calibration curve of plated glucose standards (n = 3) at zero, 0.11, 0.22, 0.33, 0.44 mM concentration. The specific molar growth yield with respect to carbon (Y_C) was determined (g dry biomass / mol C consumed).

2.4 Total Metal Analysis

Following the bacterial exposures to the test materials in oxic and anoxic conditions, respectively, the remaining volume of each test suspension/solution was harvested by centrifugation (Harrier 18/80R) for 15 min at 4500 × g. A 1.0 ml aliquot was transferred from

the resulting supernatant into a 15 ml polypropylene tube, and to which 1.0 ml of concentrated nitric acid was added. After an hour at room temperature, the contents of the tubes were digested for 2 h in a water bath set at 70 ºC. Subsequently, these digests were cooled to room temperature and diluted 1:2 with 5 % nitric acid. Total metal concentrations of silver, copper, cadmium and tellurium were then analysed by inductively coupled plasma optical emission spectrophotometry (ICP-OES, Thermo Scientific iCAP 7000 Series) or by inductively coupled plasma optical mass spectrophotometry (ICP-MS, Thermo Scientifc, X Series 2), as appropriate. Acidified, matrix-matched standard metal solutions were used for calibrations and with sample blanks included every 10 samples in each run of the instruments. The results are presented in Table 1 and Fig. S4.

2.5 Biochemistry

In order to confirm the presence of anaerobic fermentation growth (see Fig. S1), mixed-acid fermentation products were determined. The measurement of acetate concentrations (Megazyme, Éire) present in the cultures was done in polystyrene cuvettes. In triplicate, 840 µl of bacterial supernatant aliquots, blanks or standard samples, respectively, were added; followed by 200 µl of buffer and 80 µl of NAD^+ with adenosine-5′-triphosphate (ATP), coenzyme A (CoA), and polyvinylpyrollidone (PVP). NADH production was monitored at 340 nm based on a millimolar extinction coefficient. From this, acetate concentrations were determined from a calibration curve of standard solutions (n = 3) ranging from 0.02 mM to 0.5 mM acetate. Similarly, the measurement of ethanol concentrations present in the cultures was done using the Ethanol Assay Kit (Megazyme, Éire). In polystyrene cuvettes, in triplicate, 840 µl of bacterial supernatant aliquots, blanks or standard samples, respectively, were added; followed by 80 µl of buffer, 80 µl of NAD^+ and 20 µl of aldehyde dehydrogenase solution. Absorbance was determined at 340 nm after approximately 2 min at room temperature. Then, 8 µl of alcohol dehydrogenase suspension were added to the mixture. The final absorbance at 340 nm was measured after approximately 5 min. The concentration of ethanol was calculated from a calibration curve of standard solutions (n = 3) ranging from 1.1 mM to 0.1 mM ethanol concentration (Absolute ethanol standard, Sigma E7023).

A non-enzymatic colorimetric determination of formate concentrations was carried out.[30] A fresh reagent mixture consisting of 0.50 g of citric acid monohydrate (Sigma C1909, ≥ 99.0 %) and 10.0 g acetamide (Sigma 00160, ≥ 99.0 %), diluted to 100 ml with propan-2-ol (Sigma, 99.5 % HPLC grade) was prepared. Then, 1 ml of this reagent mixture was added to 0.5 ml of the bacterial supernate aliquots (n = 3), 0.05 ml of 30 % (w/v) sodium acetate (VWR,

≥ 99.0 %) and 3.5 ml acetic anhydride (Sigma 320102, ≥ 99 %) into a 6 ml propylene tube, and incubated for 2 h at room temperature; and the absorbance was then read at 515 nm. The concentration of formate was calculated from a calibration curve of standard solutions (n = 3) prepared by weighing 0.68 g sodium formate (Sigma 456020, 99.998 %) in 500 ml distilled water (20 mM) and diluted to 0 - 10 mM acid. D- and L-lactate concentrations (Megazyme, Éire) present in the bacterial supernate aliquots (n = 3) were also measured. In cuvettes, in triplicate, 840 µl of the supernatant aliquots, blanks or standard samples were added, respectively; followed by 200 µl of buffer and 80 µl of NAD^+, and 8 µl of D-glutamate-pyruvate transaminase suspension. The final absorbance reading was measured after 10 min. The concentration of D- and L-lactate was calculated from a calibration curve of standard solutions (n = 3) ranging from 0.025 mM to 0.300 mM acid.

2.6 Statistical Analyses

All data are shown as mean ± standard error of the mean (S.E.M). Following descriptive statistics, the Kolmogorov-Smirnov test was used to assess the normality of the distribution of data. Independent Student's *t*-tests and one-way analysis of variance (ANOVA, Tukey *post hoc* test) were used to check for significant differences amongst responses from within test material and treatments. In instances where the data were not found to be normally distributed, the non-parametric Mann-Whitney U test was used to assess differences between two independent groups. Likewise, the Kruskal-Wallis test was used as an alternative to a one-way between-groups analysis of variance. All statistical analyses used a 95 % confidence limit, so that p values ≥ 0.05 were not considered statistically significant. Figures were prepared using SigmaPlot 13 and statistical analyses were carried out using IBM SPSS Statistics 22.

3. Results

3.1 Total Metal in the NaCl-EBS Medium

The nominal test concentrations of each substance on a mass basis, along with the expected fraction of total metal present from each material dispersed in NaCl-EBS medium are shown (Table 1). The calculated total metal concentrations, reflect the composition of the materials and as expected, the metal concentrations are less than the mass concentration for the whole material, but provided exposures in the mg l^{-1} range. The total metal concentrations were also measured in the supernatants after the exposures (Table 1). In most cases, there was detection of total metal in the supernatants, indicating that the exposure had persisted. Inevitably, because

of adsorption and/or uptake by the test organism, and ENM aggregation in the high ionic strength media, the measured total metal in the supernatants were less than the initial dose, but consistent with our previous measurements in the same media.[22]

There were also some differences in the total metal residues in the supernatants in oxic compared to anoxic conditions (Table 1), with metal concentrations often being higher in the former. There were also some metal-specific effects on the proportion of the initial dose remaining in the supernatants. Notably for the Ag materials, the supernatants had low total Ag concentrations (Fig. S4a), in keeping with the high affinity of Ag^+ for biological ligands such as -SH. For $AgNO_3$, approximately 6 % of the initial concentration of Ag remained in the supernatants in oxic conditions, but much less for the other materials (e.g., ~ 0.3 % for the Ag bulk). Both $AgNO_3$ and Ag NPs also had less total Ag in the supernatants in anoxic compared to oxic conditions (*t*-tests, $p < 0.05$); but this was not the case for Ag bulk (Fig. S4a). For the copper treatments (Fig. S4b), between 49 – 85 % of the metal remained in the supernatants during the aerobic exposure. Some coating-effects were clear in both oxic and anoxic conditions. For example, significantly (ANOVA, $p < 0.05$) more total Cu was measured in all coated CuO NPs relative to their respective uncoated type. In anoxic conditions, all the supernatants had less total Cu than the equivalent exposure in oxic conditions (*t*-test, $p < 0.05$), except the CuO-PEG.

For the cadmium-containing test materials (Table 1), all the supernatant total Cd concentrations in anoxic conditions were statistically different from the oxic counterpart (Fig. S4c, *t*-tests, $p < 0.05$). Notably, around 39 % or more of the Cd from $CdCl_2$ remained, regardless of conditions, and the CdTe bulk material showed the least amount of Cd remaining in the supernatant (0.3 % Cd in oxic, 0.6 % Cd in anoxic conditions). There was a coating-effect, with the CdTe-NH_4^+ QDs showing less total Cd in the supernatants than the other ENMs (Fig. S4c). There were no statistical differences between oxic and anoxic conditions for total Te (*t*-tests, $p > 0.05$, Fig. S4d). Again, there was a material coating-effect with the CdTe-NH_4^+ showing the least Te remaining for the ENM exposures (Fig. S4d).

3.2 Bacterial Growth Response in the Absence of Test Materials

Following hourly measurements of *E. coli* K-12 MG1655 during aerobic and anaerobic growth, respectively, logarithmic curves were fitted to the data (Fig. S2). Aerobically, a relatively long lag phase was observed from 0 h to 8 h, followed by an exponential growth phase from 9 h to 15 h. In contrast, under anoxia, a relatively shorter lag phase was observed from 0 h to 4 h, followed by an exponential growth phase until 10 h, and a stationary phase that followed

afterwards. Nonetheless, bacterial growth was confirmed to be optimal, in terms of the calculated mean absolute biomass, in both test vessels: flasks (aerobic growth) and serum bottles (anaerobic growth), with less absolute growth measured in the latter. The percentage composition from the elemental microanalyses of *E. coli* K-12 MG1655 are shown in Fig. S3. In each case, the biomass formula for the bacterium was confirmed to be $C_{12}H_{24}O_6N_3$ (306 g $mole^{-1}$) under both oxic and anoxic conditions.

3.3 Bacterial Growth in Flasks Relative to 96-well Plates

Overall, a reproducible bacterial growth outcome was evident from most of the exposures here in flasks, as compared to the cultures in 96-well plates.[22] Nonetheless, there was more statistically significant bacterial growth inhibition in flasks as compared to plates (*t*-test, $p < 0.05$) and with the following test materials: Ag NPs, CuO-COOH NPs, CdTe-COOH, CdTe-NH_4^+ and CdTe-PEG QDs. Indeed, the results here suggest more growth inhibition in flasks *versus* the plates used in our previous study, at the same test concentrations. This apparent test-vessel effect needs further investigation. The dynamics of gas diffusion and particle behaviour could be different in the actual conical shape of the flask compared to the tubular shape in the 96-well plates. The larger flasks may allow more frequent contact between the bacterial culture and the test materials, and hence resulting in more growth inhibition. This also highlights the need for standardising apparatus for any regulatory tests with microbes and ENMs.

3.4 Percentage of Growth and Absolute Biomass in Oxic and Anoxic Conditions with Nanomaterials

Fig. 1 shows the relative percentage growth and the absolute growth as biomass compared to unexposed controls for oxic and anoxic conditions. The positive control for total bacterial growth inhibition (mercuric chloride) prevented growth at 3 mg l^{-1} nominal concentration, as expected (data not shown). Most of the materials showed statistical differences between percentage growth in oxic and anoxic conditions, and with some material-type effects, including coating-effects, within each condition (Fig. 1). Broadly, the Ag-materials had the biggest impact on growth inhibition, followed by the CdTe-containing materials, and with the Cu-containing materials generally having the least effect on growth, regardless of using oxic or anoxic conditions (Fig. 1).

Irrespective of the aeration conditions, the antibacterial response of silver (Fig. 1a) was in the order of $AgNO_3$ > Ag NPs > Ag bulk. Silver nitrate completely inhibited *E. coli* K-12 MG1655 bacterial growth, under both oxic and anoxic conditions (Fig. 1a). Similarly, Ag NPs

caused more than 99 % relative growth inhibition under both oxic and anoxic conditions (Fig. 1a). Only the Ag bulk material showed a statistical difference between the oxic and anoxic conditions, with no effect in the former and 25 % growth inhibition in the latter conditions (Fig. 1). No particle coating experiments were performed with silver because coated versions of the Ag NPs were not available, but the Ag NPs were more hazardous to percentage growth than the bulk material (Fig. 1a). The data for growth were also calculated as mean absolute biomass, and for the Ag-materials this followed a similar pattern (Fig. 1b) as the relative percentage growth.

At the 100 mg l^{-1} nominal dose of copper, $CuSO_4$ was very toxic under anoxic conditions (Fig. 1c), with > 97 % relative growth inhibition compared to 41 % in oxic conditions (*t*-test, $p < 0.05$). The CuO bulk also showed significant (*t*-test, $p < 0.05$) relative growth inhibition in anoxic conditions (> 65 %), as compared to very minimal growth inhibition (4 %) under oxic conditions (Fig. 1c). There were also some coating-effects with only the CuO-COOH and CuO-NH_4^+ materials showing statistically significant differences in relative bacterial growth (*t*-test, $p < 0.05$) between aerobic and anaerobic growth (Fig. 1c). Notably, in the anoxic conditions, all the Cu-containing ENMs enabled about 20 – 40 % more growth than the unexposed control, while the Cu salt and CuO bulk material reduced relative growth (Fig. 1c). The changes in relative growth were also reflected in absolute biomass production in the presence of the ENMs (Fig. 1d), with less absolute biomass in anoxic compared to oxic conditions; but once in anoxic conditions the CuO ENMs generally promoted biomass compared to the unexposed controls, while the metal salt and CuO bulk caused absolute biomass to decline.

For the Cd and Te-containing materials (Fig. 1e), neither of the metal salts, nor the CdTe bulk were bactericidal, with only the CdTe QDs causing growth inhibition in oxic conditions (Fig. 1e). There was also a coating-effect with the CdTe-NH_4^+ being the most toxic of the QDs in oxic conditions and causing complete inhibition of growth. In contrast, under anoxia, all of the Cd-containing substances showed some growth inhibition, and this time with a different coating-effect within the QDs, where the CdTe-COOH was the most hazardous to growth (Fig. 1e). However, there was no statistical difference in relative growth with CdTe-COOH QDs between the oxic and anoxic conditions (*t*-test, $p > 0.05$); with approximately 40 % growth inhibition in both exposure scenarios. However, the PEG-coated QDs were more harmful (*t*-test, $p < 0.05$) under oxic conditions (60 % growth inhibition) relative to the anaerobic bacterial exposure with 22 % growth inhibition (Fig. 1e). The above trends in relative growth were also reflected in the absolute measurements of biomass (Fig. 1f).

3.5 Mean Absolute Yield of Biomass in Oxic and Anoxic Conditions with Nanomaterials

The mean absolute yield of biomass per mole of carbon consumed is shown (Fig. 2). In general, absolute biomass (Fig. 1b, d and f) was reflected in the absolute yield (Fig. 2). This confirms that growth was dependent on the amount of carbon substrate used, in this case glucose. For absolute yield (Fig. 2), the situation was similar to that for relative growth (Fig. 1), with the absolute yield generally being less in anoxic conditions compared to aerobic growth. The absence of absolute biomass at the lethal doses was also reflected in zero measured absolute yields. Notably, the absolute yield tended to normalise the data, and fewer material-type or coating-effects were observed during anaerobic growth (Fig. 2a-c).

In terms of absolute yield for the silver materials, $AgNO_3$ and the Ag NPs remained the most hazardous to growth, with the Ag bulk being less biocidal than the nano-form (ANOVA, $p < 0.05$). Again, the bulk Ag was notably more toxic in anoxic *versus* oxic conditions where no effects on absolute yield were observed (Fig. 2a). For copper, the differences between yields was modest with only small biocidal effects on absolute yield in oxic conditions (Fig. 2b), but with some coating-effects between the CuO ENMs. However, absolute yield decreased in anoxic conditions, and the apparent coating-effect within the CuO ENMs was lost with no statistical differences (ANOVA, $p > 0.05$) between any of the CuO ENMs and the control (Fig. 2b).

In the presence of the CdTe bulk equivalent, the cadmium and tellurium metals salts, respectively, there was less production of absolute biomass (Fig. 1f) when compared to the normal growth control (ANOVA, $p < 0.05$); but this difference was not reflected in the absolute growth yield measurements of these materials (ANOVA, $p > 0.05$), relative to the control (Fig. 2c). There were no statistical differences between any of the Cd-containing substances on absolute yield under oxia (ANOVA, $p > 0.05$), except where the CdTe-NH_4^+ QDs completely inhibited growth. Within the anoxic conditions, only the CdTe-COOH showed a reduction in absolute yield (Fig. 2c, ANOVA, $p < 0.05$).

3.6 Products of Fermentation

The fermentation products were measured in the experiments conducted under anoxia. Fig. 3a-d shows the measured quantities of fermentation products following *E. coli* K-12 MG1655 exposure to the silver-based test materials. The measured concentrations of acetate, ethanol and formate reflected the bacterial growth inhibition during those exposures, with the lowest concentrations of fermentation products for the $AgNO_3$ (least bacterial growth), then followed by Ag NPs and Ag bulk, respectively (ANOVA, $p < 0.05$). A significant size effect was clear

between the Ag NPs and Ag bulk, where a lower concentration of acetate, ethanol and formate was measured following the former exposure (Fig. 3a-c). D- and L-lactate concentrations were only detected in the normal growth control cultures, except for L-lactate concentration detection in the $AgNO_3$ treatment, but was not different from that measured in the growth control (Fig. 3d).

The pattern of fermentation products with copper (Fig. 4a-d) reflects the observed bacterial growth pattern for these materials and the normal growth control (Fig. 1d). Such fluctuations in measured bacterial dry biomass (Fig. 1d) and fermentation metabolites (Fig. 4) is normal and within acceptable limits. The lowest quantities of acetate, ethanol and formate were measured in the presence of the copper metal salt (Fig. 4a-c). These differences (ANOVA, $p < 0.05$) were consistent relative to the growth control, the uncoated CuO NPs, the COOH- and the NH_4^+-coated NPs. There was no detection of either D- or L-lactate in the $CuSO_4$ exposure (Fig. 4d). The CuO bulk material also resulted in significant lower measured concentrations of acetate and ethanol (ANOVA, $p < 0.05$) relative to the quantities of these fermentation products measured from the growth control, the uncoated CuO NPs, the COOH- and the NH_4^+-coated NPs exposures. In general, there were few coating-effects within the fermentation products from the CuO ENM exposures, except the CuO-NH_4^+ NPs (Fig. 4a) showed a significantly higher concentration of acetate relative to the control. This corroborated earlier evidence of bacterial growth promotion (Fig. 1c) in the presence of this test material. Also, within the coated CuO ENMs, the CuO-PEG treatment has statistically less acetate and formate than the others (Fig. 4a and c, ANOVA, $p < 0.05$).

With the CdTe-based materials, the patterns of the fermentation product concentrations (Fig. 5) also reflected the observed patterns of bacterial growth with the same test materials (Fig. 1e, f). For acetate, formate and lactate, the metal salt and bulk CdTe caused concentrations to decrease compared to controls, and within the CdTe QDs there was a coating-effect with lower concentrations of fermentation products in the CdTe-COOH treatment (Fig. 5). One exception was ethanol (Fig. 5b), were none of the values in any treatment were statistically different from each other (ANOVA, $p > 0.05$).

4. Discussion

This study is one of the first to expose *E. coli* K-12 MG1655 to ENMs under both oxic and anoxic conditions. The key findings were that the majority of exposures showed different bacterial growth in oxic compared to anoxic conditions, with the latter generally being more hazardous. Notably, the metal salts and bulk materials were especially more toxic under anoxia.

There were also coating-effects within each type of ENM, but the effect was not necessarily the same in anoxic compared to oxic conditions. The measurements of fermentation products confirmed the presence of fermentation for energy production in anoxic conditions. Microbial growth measured as biomass, and bacterial growth efficiency measured as growth yield, showed that less energy is produced *via* anaerobic mixed-acid fermentation, in comparison to complete oxidation of glucose in aerobic respiration. Consequently, *E. coli* K-12 MG1655 under anoxic conditions might have less metabolic scope to manage the energetic costs of metal or nanomaterial toxicity.

4.1 Dissolved Metal Toxicity in Oxic and Anoxic Conditions

For metal species that can change oxidation state, the good aeration during the preparation of the test media will have allowed for the normal oxidised forms of the soluble metal salt controls to prevail; such as Ag^{+}, Cu^{2+}, Cd^{2+} and TeO_3^{2-}. With $AgNO_3$, at a nominal exposure concentration of 3 mg l^{-1} (0.03 mM Ag) during aerobic respiration and at a nominal exposure concentration of 6 mg l^{-1} (0.05 mM Ag) during anaerobic fermentation, toxicity (~ 100 %) was the same in oxic and anoxic conditions (Fig. 1a). This is expected, since the minimum inhibition concentration (MIC) for *E. coli* with Ag is around 0.01mM[22] to 0.06 mM[31] and the metal salt is known to be toxic at very low concentrations.[27] The mechanism of acute toxicity of dissolved silver to *E. coli* includes inhibiting the respiratory chain[32] and interference with DNA replication to prevent bacterial growth.[33] In anoxic conditions in soil, Ag^{+} from $AgNO_3$ can be reduced to the insoluble metallic Ag°,[34] or relatively inert Ag_2S particles when sulfide is present.[35] However, in the EBS-NaCl media, the high ionic strength will drive sparingly soluble silver chloride complexation. The calculated species present were: Ag^{+} 0.027 %, AgCl (aq) 5.0 %, $AgCl_2^{-}$ 75.2 %, and $AgCl_3^{2-}$ 19.8 % (Visual MINTEQ version 3.1). Consequently, $AgNO_3$ is instantaeously transformed to silver chloride-containing NPs in such salines with only a tiny fraction of Ag^{+} remaining.[10] Since there was no added sulfide, the same speciation will occur in anoxic conditions, and hence in both exposures the toxicity potential is the same.

During aerobic growth, $CuSO_4$ at a nominal exposure concentration of 100 mg l^{-1} (1 mM Cu) caused 10 – 40 % growth inhibition (Fig. 1c). This was also as expected, since the *E. coli* MIC for Cu^{2+} ranges from > 1mM[22] to 4.5 mM.[31] Under anoxia, the Cu metal salt was found to be highly toxic, showing > 97 % bacterial growth inhibition (Fig. 1c). When oxygen is very limited, copper is known to become reduced from Cu^{2+} to Cu^{+} and the metal becomes even more toxic to *E. coli* cells; as it is the Cu^{+} form that is taken up through biological

membranes.[36] Cu(I) inhibits the Fe–S-containing dehydratases involved in amino acid synthesis and interferess with the metabolic functioning of *E. coli* cells.[27]

Despite appearing very soluble in the EBS-NaCl growth medium (Table 1), the cadmium and tellurium metal salts were not toxic here under oxic conditions, while in anoxic conditions bacterial growth was reduced by 30 – 40 % (Fig. 1e). With respect to the cadmium metal salt, the test concentration used here (3 mg l^{-1} nominal exposure concentration, 0.01 mM Cd) was about a 100-fold less than the Cd^{2+} MIC for *E. coli* at 1.1 mM.[31] An MIC value of more than 0.34 mM Cd has also been reported for *E. coli* during aerobic growth in 96-well plates.[22] The toxicity of Cd (II) ions has often been synonymous with its high affinity for binding to sulfhydryl (R-SH) protein-containing groups, causing oxidation and depletion of cellular thiol groups with the resulting consequences of protein denaturation.[27] Speciation calculations showed a good proportion of Cd^{2+} in the media: Cd^{2+} 12.2 %, $CdCl^{+}$ 61.9 %, $CdCl_2$ (aq) 23.3 % and $CdHPO_4$ (aq) 2.7 % (Visual MINTEQ version 3.1). Tellurite speciation is challenging to calculate as the stability constants are not agreed. Nonetheless, the metalloid oxyanion in potassium tellurite (TeO_3^{2-}) causes oxidative stress in most bacterial species.[37] In aerated 96-well plates, bacterial growth inhibition in the presence of potassium tellurite was observed to be dose-dependent.[22] Bacteria, including *E. coli*, can regulate the presence of the tellurite anion intracellularly by reducing Te^{4+} to insoluble elemental and non-toxic black Te°.[38] This metal detoxification approach was also evident here with *E. coli* K-12 MG1655. Incidental visual observation at the end of the bacterial incubation period confirmed the presence of black particles within the test suspensions following the tellurite exposures, in both aerobic and anaerobic growth. Parallel incubation of control flasks with K_2TeO_3 in the absence of the bacterial inoculum, did not result in the formation of the black metallic deposit.

4.2 Are There Particle Size Effects and Are They Different in Anoxic Conditions?

In terms of comparing ENMs with their micron scale counterparts, under oxia, the bulk material for Ag, CuO and CdTe were not appreciably bactericidal (Fig. 1). Similar observations were made in experiments carried out in 96-well plates with the same materials.[22] The bulk materials should, in theory, be less reactive than the nanoscale equivalents, where the latter have a larger surface area to volume ratio and with more reactive surfaces at the nano scale. For example, with the bulk form of silver, the amount of ionic species available for surface reactivity is restricted, unlike in the nano form of the same metal.[39] The Ag bulk and the CdTe bulk inherently also displayed minimal dissolution in the EBS-NaCl growth medium;[22] as seen from measurements of total metal concentration here (Fig. S4) following both aerobic and anaerobic

bacterial growth. To some extent, one could argue that being insoluble would make the bulk materials even less hazardous to the bacterial test suspensions. It is therefore unclear from chemical properties alone why the bulk materials were generally bactericidal to *E. coli* K-12 MG1655 grown under anoxic conditions. However under anoxia, enzyme-mediated reduction of metal oxides by microbes can cause dissolution.[40]

For the Ag NPs, the measured bacterial growth did not differ between oxic and anoxic conditions (Fig. 1a, b). This material is known to be toxic to bacteria,[39] with a MIC value (0.06 mM) equal to that of Hg^{2+}.[31] It appears that oxygen was not a limiting factor in the toxicity (Fig. 1a, b). Studies with Ag NPs on the early phases of bacterial biofilm formation, observed less *E. coli* cells adherence during both aerobic and anaerobic growth.[18] Despite showing minimal dissolution in the EBS-NaCl growth medium[22], there was 0.2 – 0.4 % measured total silver from Ag NPs (Fig. S4). In anoxic conditions, any Ag^{+} released by dissolution is not toxic to bacteria *via* oxidative stress because there is no oxygen.[17] Instead, the high affinity of the Ag^{+}, or the Ag NPs, with ligands in the organism (phosphated or sulfated ligands on proteins, etc.,) may be enough to drive toxicity.[17] In the conditions here, the formation of insoluble and less toxic Ag_2S NPs is likely to be limited because there was only incidental sulfur sources (~0.4 mM from $MgSO_4$) in the media. The bacterial growth responses of CuO and CdTe ENMs are discussed in the next section in context with the coating-effects.

4.3 Are There Coating-Effects Within ENMs and Do They Differ in Anoxic Conditions?

In terms of a coating-mediated effect with the CuO ENMs in oxic conditions, only the carboxyl-coated CuO NPs caused a significant reduction in bacterial growth relative to the control (Fig. 1c, d). Dissolution experiments on these same test materials have shown that the ENM coatings do increase the release of dissolved Cu by a few percent.[22] Despite this, in aerated 96-well plates, the CuO ENMs, both coated and uncoated, were not found to be bactericidal[22] up to a nominal concentration of 100 mg l^{-1}. Interestingly, under anoxia, the uncoated, COOH- and ammonium-coated CuO NPs, respectively, led to an increase in absolute biomass production (Fig. 1d) and absolute yield (Fig. 2b), relative to the growth control. Thus, in the anoxic conditions adopted here at 100 mg l^{-1} nominal exposure concentration (uncoated CuO NPs containing 1 mM Cu; CuO COOH NPs containing 0.6 mM Cu, CuO NH_4^{+} NPs containing 0.7 mM Cu and CuO PEG NPs containing 0.4 mM Cu), the CuO NPs improved growth, irrespective of the type of coating. This might be a hormetic effect associated with the early induction of metal binding proteins as is the case for copper salts.[41] Any apparent Cu resistance associated with CuO NPs requires further investigation.

In oxic conditions, unlike their bulk semiconductor form, the CdTe QDs were confirmed to be highly bactericidal (Fig. 1e). The CdTe QDs have electron confinement in all three spatial configurations.[42] This causes higher bandgap energy[43] leading to the harmful production of free radicals in aqueous solutions, but only when oxygen as a precursor is present. Consequently in aerobic growth QDs may be toxic *via* lipid peroxidation of the bacterial cell membrane.[44] However, the toxicity is also coating-dependent. In this study, aerobically, growth inhibition was most severe in the presence of the CdTe-NH_4^+ QDs form, followed by the carboxylate and the PEG-coated form (Fig. 1e, f). Similar to our previous finding using aerobic growth.[22] In contrast, in anoxic conditions, the QDs were generally much less toxic with only partial growth inhibition (~ 20 %), except for the COOH-coated QDs that caused an equal growth inhibition effect (60 %) with and without oxygen presence (Fig. 1e, f). The surface coatings on the QDs might have influenced the particle behaviour, but with the organism having a net negative charge one might expect the postively charged CdTe-NH_4^+ QDs to be attracted to the bacterial cell surface. There is no clear mechanistic explanation for the observed coating-effects here. In the earthworm *Eisenia fetida* (Savigny 1826), there were also inconsistent trends in toxicity ranking following exposures to the differently coated CdTe QDs used here that were not readily explained by dissolution or other ENM behaviours.[45] Human *in vitro* toxicological studies using the same CdTe QDs batches, found these materials to be cytotoxic, irrespective of the surface coating form.[46] So, the coating-effects are also dependent on the type of test organism.

4.4 Products of Fermentation

The anaerobic bacterial growth patterns (Fig. 1, 2) were reflected in the measured concentrations of the fermentation products (Fig. 3 - 5). The test materials could be classified by their scope of fermentation; whereby the most bactericidal test materials resulted in the least fermentation. For example, Ag NPs were observed to be more toxic than the microscale Ag material (Fig. 1a, b). This was reflected in lower concentrations of measured respiratory products with Ag NPs (Fig. 3a, c) in comparison with bulk Ag.

E. coli cells can regulate the formation of CO_2 and the concentration of acidic fermentation products in their growth environment, that may otherwise inhibit cell survival in a highly acidic medium.[47] In aerobic growth, the pH of the medium did not decrease below pH 5.6, whereas anaerobically the pH of the medium decreased to a final lowest pH of 5.2 (data not shown). Arguably, the decrease in pH during fermentation could have contributed to an increase in free metal ion concentrations within the supernatants due to dissolution. However, metal concentrations in the supernatants did not increase for silver, copper and tellurium (Fig.

S4a, b and d). The cadmium-containing test materials, namely CdTe bulk, $CdCl_2$, CdTe-COOH and CdTe-PEG QDs, measured statistically significant higher cadmium concentrations anaerobically relative to the aerobic counterparts (Table 1); and with more total Cd in the supernatants (Fig. S4c). But this would not increase the proportion of dissolved and particulate cadmium in the EBS-NaCl media used here in anoxic conditions. For example, the proportion of Cd^{2+} species was calculated as 12.2, 12.5, and 12.5 % at pH 7, 5.6 and 5.2 respectively (Visual MINTEQ version 3.1). The presence of more dissolved cadmium ions in the anoxic test media (Fig. S4c) was likely responsible for instances with less absolute growth measured relative to the unexposed control (Fig. 1f), and possibly also the apparent coating-effect.

Metals are known to have a strong affinity for naturally occurring organic matter and negatively charged ligands.[21, 48] However, the metabolites themselves, are unlikely to influence metal bioavailability here. The fermentation products acetic acid, formic acid and lactic acid, have one carboxyl acid group in their structure (Fig. S1). At the pH range of the anaerobic bacterial culture medium (pH 5.2 – 6.7), these acids tend to be in their carboxylate anion state. Stability constants of less than two have been measured for formate and acetate, respectively, in the presence of Cu^{2+} or Cd^{2+}.[49] These affinity values are considered low;[50] with very weak complexation with transitional metal ions (e.g., Cu^{2+}).

4.5 Metabolic Costs of Toxicity

Microbes have well-known mechanisms for the homoeostatic control of essential metals and managing the toxicity of non-essential dissolved metals, for example, by the induction of metal binding ligands.[27, 31] In order to ensure a probabilty of survival in the long term, the metabolic scope of the organism must be able to meet the cost of metal toxicity. Thus, in the presence of excessive metal concentrations, a continual good supply of energy is essential for bacterial growth. In this study, bacterial growth inhibition in the presence of Ag, Cu and CdTe, respectively, was in general more severe under anaerobic relative to aerobic growth (Fig. 1); suggesting that decreased metabolic scope was limiting growth. This was also observed in the presence of Fe° NPs.[20] As a facultative microbe *E. coli* K-12 MG1655 can produce energy *via* complete or partial (mixed-acid fermentation) oxidation of glucose (Fig. S1). Typically for members of the phylum *Pseudomonadota* (such as *Escherichia* spp.) growing by respiration of glucose, around 50 – 60 % of glucose-carbon is assimilated into biomass and 40 – 50 % is dissimilated to CO_2 for generation of ATP/reducing equivalents; however, during glucose fermentation, only 1 – 5 % of glucose-carbon is assimilated and 95 – 99 % is dissimilated into CO_2 and fatty acids and alcohols for generation of ATP/regeneration of $NAD(P)^+$.[51] In other

words, the bacteria had 20 times as much energy available to deal with metal or ENM exposure during oxic conditions, and so these conditions are generally less toxic (for calculation details, see Supplementary Material).

4.6 Environmental Implications

Bacteria are extensively used in regulatory testing for environmental hazard assessment of chemicals.[26] A few regulatory tests are specifically directed to microbes living in the soil. Amongst these, the Organisation for Economic Co-operation and Development (OECD) Test No. 216 and 217 measure microbial nitrogen and carbon transformations in soil. These two tests have been used in the presence of Ag and TiO_2 NPs, and modification to these protocols have been proposed to better adapt the tests for ENM exposures.[52] OECD Test No. 303A was also adapted to investigate the effects of TiO_2 NPs on the biodegradation and nitrification of sewage sludge and effluents.[53] However, for the soil tests especially, these are usually conducted in oxic conditions where the soil has been mixed. In contrast, an undisturbed natural soil will be stratified and with less oxygenated layers deeper down in the soil. The findings here suggest that the ENMs are generally more toxic in anoxic conditions to *E. coli* K-12 MG1655, and also for some of the metal salt and bulk materials. Consequently, the current OECD tests may underestimate the hazard to microbes and their functions in soils/sediments.

A second concern is whether the existing risk assessments for dissolved metals will adequately protect for the nano form. During both aerobic and anaerobic growth, the metal salts of Ag and Cu were found to be more bactericidal than the corresponding nano forms (Fig. 1a, c). In contrast, the QDs were more harmful (Fig. 1e) than the cadmium and tellurium metal salt, irrespective of the aeration conditions. The coated CdTe QDs were previously found to be more bactericidal than their metal salts equivalent, following *E. coli* K-12 MG1655 aerobic growth.[22] This would imply that the existing metal risk assessments for cadmium and tellurium might not be protective enough from environmental releases of QDs. Detrimental effects from metal toxicity burden can lead to less fertile soils.[54] Albeit so far, such consequences on soil microbial communities were minimal.[55]

5. Conclusion

In this work, the facultative *E. coli* K-12 MG1655 was observed to be more negatively affected by the presence of Ag, Cu and CdTe during mixed-acid fermentation, as compared to aerobic respiration; particularly for the bulk test materials and their equivalent metal salts. The reduction in metabolic scope during anoxic conditions limited bacterial growth, and increased

667 the disposition of the organism to toxicity. The detection of fermentation products in the media
668 confirmed anaerobic growth, and still occurred as expected in the presence of ENMs. The Ag
669 materials were most bactericidal, followed by the Cd-containing materials, regardless of oxic
670 or anoxic conditions. Coating-effects were observed in both Cu and CdTe ENMs; but were not
671 readily explained by known aspects of metal dissolution or other particle properties and
672 behaviours. This study highlights that the toxicity of ENMs to microbes, such as *E. coli* K-12
673 MG1655, can be greater in anoxic conditions. Arguably, it would be prudent to also conduct
674 some regulatory tests with microbes, along an oxygen concentration gradient and with chemical
675 dose response curves, to better support hazard assessment. Or at least, include safety factors for
676 the extrapolation from oxic to anoxic conditions in the ecosystem for environmental risk
677 assessment purposes. Only a few ENMs are explored here, and further research on other types
678 of ENMs is needed to have an in-depth understanding of the hazards of EMNs to facultative
679 microbes. This would include more knowledge of how ENMs are transformed with the dynamic
680 changes in oxygenation in water, soils and sediments.
681
682 **Author contributions**
683 RB proposed the initial experimental design. JV conducted the experiments that provided all
684 the data sets used here. Manuscript preparation and writing of the drafts was led by RDH, with
685 JV preparing the data illustrations, main text and statistics, and RB providing the energy change
686 calculations. All the co-authors read subsequent drafts.
687
688 **Acknowledgements**
689 Kind thanks to Dr Alexey Kalachev (PlasmaChem GmbH, http://www.plasmachem.com/) for
690 providing most of the coated-ENMs and their associated core materials. This work was funded
691 by the European Commission, under grant agreement FP7-309329 (NANOSOLUTIONS), with
692 RDH as the principle investigator at UoP.
693
694 **Conflict of Interest**
695 The authors report no conflicts of interest. The authors alone are responsible for the content and
696 writing of the paper.
697
698
699

References

1. H. W. Paerl and J. L. Pinckney, A mini-review of microbial consortia: Their roles in aquatic production and biogeochemical cycling, *Microbial Ecology*, 1996, **31**, 225-247.
2. R. M. Soo, J. Hemp, D. H. Parks, W. W. Fischer and P. Hugenholtz, On the origins of oxygenic photosynthesis and aerobic respiration in Cyanobacteria, *Science*, 2017, **355**, 1436-1440.
3. B. B. Jørgensen, in *Marine Geochemistry*, eds. H. D. Schulz and M. Zabel, Springer Berlin Heidelberg, Berlin, Heidelberg, 2000, DOI: 10.1007/978-3-662-04242-7_5, pp. 173-207.
4. K. Hartman and S. G. Tringe, Interactions between plants and soil shaping the root microbiome under abiotic stress, *Biochemical Journal*, 2019, **476**, 2705-2724.
5. T. Y. Sun, N. A. Bornhöft, K. Hungerbühler and B. Nowack, Dynamic probabilistic modeling of environmental emissions of engineered nanomaterials, *Environmental Science and Technology*, 2016, **50**, 4701-4711.
6. B. Giese, F. Klaessig, B. Park, R. Kaegi, M. Steinfeldt, H. Wigger, A. von Gleich and F. Gottschalk, Risks, release and concentrations of engineered nanomaterial in the environment, *Scientific Reports*, 2018, **8**, 1565.
7. J. D. Judy, J. K. Kirby, C. Creamer, M. J. McLaughlin, C. Fiebiger, C. Wright, T. R. Cavagnaro and P. M. Bertsch, Effects of silver sulfide nanomaterials on mycorrhizal colonization of tomato plants and soil microbial communities in biosolid-amended soil, *Environmental Pollution*, 2015, **206**, 256-263.
8. A. Praetorius, A. Gundlach-Graham, E. Goldberg, W. Fabienke, J. Navratilova, A. Gondikas, R. Kaegi, D. Günther, T. Hofmann and F. von der Kammer, Single-particle multi-element fingerprinting (spMEF) using inductively-coupled plasma time-of-flight mass spectrometry (ICP-TOFMS) to identify engineered nanoparticles against the elevated natural background in soils, *Environmental Science: Nano*, 2017, **4**, 307-314.
9. O. M. Bondarenko, M. Heinlaan, M. Sihtmäe, A. Ivask, I. Kurvet, E. Joonas, A. Jemec, M. Mannerström, T. Heinonen, R. Rekulapelly, S. Singh, J. Zou, I. Pyykkö, D. Drobne and A. Kahru, Multilaboratory evaluation of 15 bioassays for (eco)toxicity screening and hazard ranking of engineered nanomaterials: FP7 project NANOVALID, *Nanotoxicology*, 2016, **10**, 1229-1242.
10. A. Besinis, T. De Peralta and R. D. Handy, The antibacterial effects of silver, titanium dioxide and silica dioxide nanoparticles compared to the dental disinfectant

chlorhexidine on *Streptococcus mutans* using a suite of bioassays, *Nanotoxicology*, 2014, **8**, 1-16.

11. X. Sun, M. Dong, Z. Guo, H. Zhang, J. Wang, P. Jia, T. Bu, Y. Liu, L. Li and L. Wang, Multifunctional chitosan-copper-gallic acid based antibacterial nanocomposite wound dressing, *International Journal of Biological Macromolecules*, 2021, **167**, 10-22.

12. J. D. Fortner, D. Y. Lyon, C. M. Sayes, A. M. Boyd, J. C. Falkner, E. M. Hotze, L. B. Alemany, Y. J. Tao, W. Guo, K. D. Ausman, V. L. Colvin and J. B. Hughes, C_{60} in water: Nanocrystal formation and microbial response, *Environmental Science and Technology*, 2005, **39**, 4307-4316.

13. A. A. Taylor, G. M. Aron, G. W. Beall, N. Dharmasiri, Y. Zhang and R. J. C. McLean, Carbon and clay nanoparticles induce minimal stress responses in gram negative bacteria and eukaryotic fish cells, *Environmental Toxicology*, 2014, **29**, 961-968.

14. X. Zou, P. Li, X. Wang, S. Zheng, F. Dai and H. Zhang, Silver nanoparticle and Ag^{+}-induced shifts of microbial communities in natural brackish waters: Are they more pronounced under oxic conditions than anoxic conditions?, *Environmental Pollution*, 2020, **258**, 113686.

15. B. Demirel, The impacts of engineered nanomaterials (ENMs) on anaerobic digestion processes, *Process Biochemistry*, 2016, **51**, 308-313.

16. J. Gonzalez-Estrella, D. Puyol, S. Gallagher, R. Sierra-Alvarez and J. A. Field, Elemental copper nanoparticle toxicity to different trophic groups involved in anaerobic and anoxic wastewater treatment processes, *Science of The Total Environment*, 2015, **512-513**, 308-315.

17. Z.-M. Xiu, J. Ma and P. J. J. Alvarez, Differential effect of common ligands and molecular oxygen on antimicrobial activity of silver nanoparticles *versus* silver ions, *Environmental Science and Technology*, 2011, **45**, 9003-9008.

18. E. Garuglieri, C. Catto, F. Villa, R. Zanchi and F. Cappitelli, Effects of sublethal concentrations of silver nanoparticles on *Escherichia coli* and *Bacillus subtilis* under aerobic and anaerobic conditions, *Biointerphases*, 2016, **11**, 04B308.

19. F. Dong and Y. Zhou, Differential transformation and antibacterial effects of silver nanoparticles in aerobic and anaerobic environment, *Nanotoxicology*, 2019, **13**, 339-353.

20. Q. Xie, L. Li, H. Dong, R. Li, R. Tian and J. Chen, Influence of several crucial groundwater components on the toxicity of nanoscale zero-valent iron towards

Escherichia coli under aerobic and anaerobic conditions, *Chemosphere*, 2021, **285**, 131453.

21. G. You, Y. Xu, P. Wang, C. Wang, J. Chen, J. Hou, L. Miao, Y. Gao and Y. Li, Deciphering the effects of CeO_2 nanoparticles on *Escherichia coli* in the presence of ferrous and sulfide ions: Physicochemical transformation-induced toxicity and detoxification mechanisms, *Journal of Hazardous Materials*, 2021, **413**, 125300.
22. J. Vassallo, A. Besinis, R. Boden and R. D. Handy, The minimum inhibitory concentration (MIC) assay with *Escherichia coli*: An early tier in the environmental hazard assessment of nanomaterials?, *Ecotoxicology and Environmental Safety*, 2018, **162**, 633-646.
23. V. Khanh Nguyen, D. Kumar Chaudhary, R. Hari Dahal, N. Hoang Trinh, J. Kim, S. W. Chang, Y. Hong, D. Duc La, X. C. Nguyen, H. Hao Ngo, W. J. Chung and D. D. Nguyen, Review on pretreatment techniques to improve anaerobic digestion of sewage sludge, *Fuel*, 2021, **285**, 119105.
24. N. A. Yasid, M. D. Rolfe, J. Green and M. P. Williamson, Homeostasis of metabolites in *Escherichia coli* on transition from anaerobic to aerobic conditions and the transient secretion of pyruvate, *Royal Society Open Science*, 2016, **3**, 160187.
25. S. Steinsiek, S. Frixel, S. Stagge and K. Bettenbrock, Characterization of *E. coli* MG1655 and frdA and sdhC mutants at various aerobiosis levels, *Journal of Biotechnology*, 2011, **154**, 35-45.
26. M. Crane, R. D. Handy, J. Garrod and R. Owen, Ecotoxicity test methods and environmental hazard assessment for engineered nanoparticles, *Ecotoxicology*, 2008, **17**, 421.
27. J. A. Lemire, J. J. Harrison and R. J. Turner, Antimicrobial activity of metals: mechanisms, molecular targets and applications, *Nature Reviews Microbiology*, 2013, **11**, 371-384.
28. J. B. A. Dumas, Procedes de l'analyse organique, *Ann. Chim. Phys*, 1831, **247**, 198-213.
29. J. Unterzaucher, The direct micro-determination of oxygen in organic substances, *Analyst* 1952, **77**, 584-595.
30. E. Lang and H. Lang, Spezifische Farbreaktion zum direkten Nachweis der Ameisensäure, *Fresenius' Zeitschrift für analytische Chemie*, 1972, **260**, 8-10.
31. J. J. Harrison, H. Ceri, C. A. Stremick and R. J. Turner, Biofilm susceptibility to metal toxicity, *Environmental Microbiology*, 2004, **6**, 1220-1227.

802 32. P. D. Bragg and D. J. Rainnie, The effect of silver ions on the respiratory chain of
803 *Escherichia coli*, *Canadian Journal of Microbiology*, 1974, **20**, 883-889.
804 33. S. Silver, L. T. Phung and G. Silver, Silver as biocides in burn and wound dressings
805 and bacterial resistance to silver compounds, *Journal of Industrial Microbiology and*
806 *Biotechnology*, 2006, **33**, 627-634.
807 34. Y. Hashimoto, S. Takeuchi, S. Mitsunobu and Y.-S. Ok, Chemical speciation of silver
808 (Ag) in soils under aerobic and anaerobic conditions: Ag nanoparticles vs. ionic Ag,
809 *Journal of Hazardous Materials*, 2017, **322**, 318-324.
810 35. J. R. Lead, G. E. Batley, P. J. J. Alvarez, M.-N. Croteau, R. D. Handy, M. J.
811 McLaughlin, J. D. Judy and K. Schirmer, Nanomaterials in the environment:
812 Behavior, fate, bioavailability, and effects—An updated review, *Environmental*
813 *Toxicology and Chemistry*, 2018, **37**, 2029-2063.
814 36. P. H. Beswick, G. H. Hall, A. J. Hook, K. Little, D. C. H. McBrien and K. A. K. Lott,
815 Copper toxicity: Evidence for the conversion of cupric to cuprous copper *in vivo* under
816 anaerobic conditions, *Chemico-Biological Interactions*, 1976, **14**, 347-356.
817 37. J. Sandoval, F. Arenas, J. García, W. Díaz-Vásquez, M. Valdivia-González, M.
818 Sabotier and C. Vásquez, *Escherichia coli* 6-phosphogluconate dehydrogenase aids in
819 tellurite resistance by reducing the toxicant in a NADPH-dependent manner,
820 *Microbiological Research*, 2015, **177**, 22-27.
821 38. J. M. Pérez, I. L. Calderón, F. A. Arenas, D. E. Fuentes, G. A. Pradenas, E. L. Fuentes,
822 J. M. Sandoval, M. E. Castro, A. O. Elías and C. C. Vásquez, Bacterial toxicity of
823 potassium tellurite: unveiling an ancient enigma, *PloS one*, 2007, **2**, e211.
824 39. B. Reidy, A. Haase, A. Luch, K. A. Dawson and I. Lynch, Mechanisms of silver
825 nanoparticle release, transformation and toxicity: A critical review of current
826 knowledge and recommendations for future studies and applications, *Materials*, 2013,
827 **6**, 2295-2350.
828 40. A. Francis and C. Dodge, Anaerobic microbial dissolution of transition and heavy
829 metal oxides, *Applied and Environmental Microbiology*, 1988, **54**, 1009-1014.
830 41. A. R. D. Stebbing, Hormesis — The stimulation of growth by low levels of inhibitors,
831 *Science of The Total Environment*, 1982, **22**, 213-234.
832 42. M. S. Giroux, Z. Zahra, O. A. Salawu, R. M. Burgess, K. T. Ho and A. S. Adeleye,
833 Assessing the environmental effects related to quantum dot structure, function,
834 synthesis and exposure, *Environmental Science: Nano*, 2022, DOI:
835 10.1039/D1EN00712B.

43. S. Nikazar, V. S. Sivasankarapillai, A. Rahdar, S. Gasmi, P. S. Anumol and M. S. Shanavas, Revisiting the cytotoxicity of quantum dots: an in-depth overview, *Biophysical Reviews*, 2020, **12**, 703-718.
44. E. Dumas, V. Ozenne, R. E. Mielke and J. L. Nadeau, Toxicity of CdTe quantum dots in bacterial strains, *IEEE Transactions on NanoBioscience*, 2009, **8**, 58-64.
45. K. Tatsi, T. H. Hutchinson and R. D. Handy, Consequences of surface coatings and soil ageing on the toxicity of cadmium telluride quantum dots to the earthworm *Eisenia fetida*, *Ecotoxicology and Environmental Safety*, 2020, **201**, 110813.
46. A. Gallud, M. Delaval, P. Kinaret, V. S. Marwah, V. Fortino, J. Ytterberg, R. Zubarev, T. Skoog, J. Kere, M. Correia, K. Loeschner, Z. Al-Ahmady, K. Kostarelos, J. Ruiz, D. Astruc, M. Monopoli, R. Handy, S. Moya, K. Savolainen, H. Alenius, D. Greco and B. Fadeel, Multiparametric profiling of engineered nanomaterials: Unmasking the surface coating effect, *Advanced Science*, 2020, **7**, 2002221.
47. D. Blankenhorn, J. Phillips and J. L. Slonczewski, Acid- and base-induced proteins during aerobic and anaerobic growth of *Escherichia coli* revealed by two-dimensional gel electrophoresis, *J Bacteriol*, 1999, **181**, 2209-2216.
48. J. E. Scott, Affinity, competition and specific interactions in the biochemistry and histochemistry of polyelectrolytes, *Biochemical Society Transactions*, 1973, **1**, 787-806.
49. J. W. Bunting and K. M. Thong, Stability constants for some 1:1 metal–carboxylate complexes, *Canadian Journal of Chemistry*, 1970, **48**, 1654-1656.
50. H. Okochi and P. Brimblecombe, Potential trace metal–organic complexation in the atmosphere, *The Scientific World Journal*, 2002, **2**, 356173.
51. S. J. Pirt, *Principles of Microbe and Cell Cultivation*, Blackwell, London, 1975.
52. K. Hund-Rinke, A. Baun, D. Cupi, T. F. Fernandes, R. Handy, J. H. Kinross, J. M. Navas, W. Peijnenburg, K. Schlich, B. J. Shaw and J. J. Scott-Fordsmand, Regulatory ecotoxicity testing of nanomaterials – proposed modifications of OECD test guidelines based on laboratory experience with silver and titanium dioxide nanoparticles, *Nanotoxicology*, 2016, **10**, 1442-1447.
53. S. Gartiser, F. Flach, C. Nickel, M. Stintz, S. Damme, A. Schaeffer, L. Erdinger and T. A. J. Kuhlbusch, Behavior of nanoscale titanium dioxide in laboratory wastewater treatment plants according to OECD 303 A, *Chemosphere*, 2014, **104**, 197-204.

54. S. P. McGrath, A. M. Chaudri and K. E. Giller, Long-term effects of metals in sewage sludge on soils, microorganisms and plants, *Journal of Industrial Microbiology*, 1995, **14**, 94-104.
55. M. Durenkamp, M. Pawlett, K. Ritz, J. A. Harris, A. L. Neal and S. P. McGrath, Nanoparticles within WWTP sludges have minimal impact on leachate quality and soil microbial community structure and function, *Environmental Pollution*, 2016, **211**, 399-405.

Table 1. Characterisation details of the test materials, with nominal test exposure concentrations in 0.90 % NaCl, along with the pre-exposure calculated total metal concentrations in the NaCl-EBS medium, and post-bacterial exposure measured total metal concentrations, following aerobic and anaerobic growth, respectively.

Test material (supplier)	Manufacturer's information [g]	Aerobic growth				Anaerobic growth			
		Nominal test exposure concentration in 0.90 % NaCl (mg l^{-1})	Pre-exposure calculated total metal concentration dosed in NaCl-EBS medium (mg l^{-1})	Measured metal concentration in the supernatant post-bacterial exposure (mg l^{-1}) [b]	Between-replicate percentage coefficient of variation (%)	Nominal test exposure concentration (mg l^{-1})	Pre-exposure calculated total metal concentration dosed in NaCl-EBS medium (mg l^{-1})	Measured metal concentration in the supernatant post-bacterial exposure (mg l^{-1}) [b]	Between-replicate percentage coefficient of variation (%)
Ag Bulk, CAS 7440-22-4 (Sigma-Aldrich 327085, Lot MKBR8201V)	Diameter, 2 - 3.5 µm; purity ≥ 99.9 % trace metal basis	3	2.63 Ag	0.001 ± 0.00004 Ag	7.8	6	5.27 Ag	0.002 ± 0.001 Ag	51.5
$AgNO_3$, CAS 7761-88-8 (BDH Chemicals)	0.10 M volumetric solution, certified	3	2.78 Ag	0.157 ± 0.001 Ag	1.2	6	5.55 Ag	0.106 ± 0.001 Ag [d]	1.4
Ag NPs, with PVP dispersant, CAS 7440-22-4 (Sigma-Aldrich 576832, Lot 7721KH)	Diameter, < 100 nm; purity, 99.5 % trace metals basis; Fisher sub-sieve sizer surface area, 5.0 m^2 g^{-1}	3	2.64 Ag	0.012 ± 0.0003 Ag	4.4	6	5.28 Ag	0.012 ± 0.002 Ag	24.2
CuO Bulk, CAS 1317-38-0 (British Drug Houses Ltd)	Analar grade	100	66.4 Cu	32.24 ± 0.481 Cu	2.6	100	66.4 Cu	28.88 ± 0.298 Cu [d]	1.8
$CuSO_4.5H_2O$, CAS 7758-99-8 (Sigma-Aldrich 31293 , Lot SZBC0170V)	Purity, 99 - 102 %	100	65.5 Cu	56.80 ± 0.436 Cu	1.3	100	65.5 Cu	49.56 ± 0.396 Cu [d]	1.4

Test material (supplier)	Manufacturer's information [g]	Aerobic growth				Anaerobic growth			
		Nominal test exposure concentration in 0.90 % NaCl (mg l^{-1})	Pre-exposure calculated total metal concentration dosed in NaCl-EBS medium (mg l^{-1})	Measured metal concentration in the supernatant post-bacterial exposure (mg l^{-1}) [b]	Between-replicate percentage coefficient of variation (%)	Nominal test exposure concentration (mg l^{-1})	Pre-exposure calculated total metal concentration dosed in NaCl-EBS medium (mg l^{-1})	Measured metal concentration in the supernatant post-bacterial exposure (mg l^{-1}) [b]	Between-replicate percentage coefficient of variation (%)
CuO NPs uncoated, CAS 1317-38-0 (PlasmaChem GmbH, Lot YF1309121) [a]	Diameter, 10 - 20 nm; surface area, 42 ± 2 m^2 g^{-1}; zeta potential, 14.0 ± 1.2 mV	100	66.4 Cu	33.10 ± 0.372 Cu	1.9	100	66.4 Cu	16.48 ± 1.528 Cu [d]	16.1
CuO NPs COOH-coated, CAS 1317-38-0 (PlasmaChem GmbH, Lot YF140114) [a]	Diameter, 10 - 20 nm; surface area, 7.4 ± 0.5 m^2 g^{-1}; zeta potential, -7.3 ± 0.5 mV	100	35.7 Cu	24.97 ± 0.554 Cu	3.8	100	35.7 Cu	19.63 ± 0.564 Cu [d]	5.0
CuO NPs NH_4^+-coated, CAS 1317-38-0 (PlasmaChem GmbH, Lot 140114) [a]	Diameter, 10 - 20 nm; surface area, 6.1 ± 0.5 m^2 g^{-1}; zeta potential, 27.7 ± 0.5 mV	100	43.2 Cu	29.86 ± 0.477 Cu	2.8	100	43.2 Cu	22.84 ± 0.188 Cu [d]	1.4
CuO NPs PEG-coated, CAS 1317-38-0 (PlasmaChem GmbH, Lot YF140114) [a]	Diameter, 10 - 20 nm; zeta potential, -16.8 ± 0.4 mV	100	24.1 Cu	20.00 ± 0.799 Cu	6.9	100	24.1 Cu	19.37 ± 0.245 Cu	2.2
CdTe Bulk, CAS 1306-25-8 (Sigma-Aldrich 256544, Lot MKBK6448V)	Diameter, < 250 µm; purity, ≥ 99.99 % trace metal basis	3	1.23 Cd 1.38 Te	0.004 ± 0.0001 Cd 0.004 Te [c]	6.5 [f]	3	1.23 Cd 1.38 Te	0.007 ± 0.0001 Cd [d] 0.004 Te [c]	2.6 [f]

Test material (supplier)	Manufacturer's information [g]	Aerobic growth				Anaerobic growth			
		Nominal test exposure concentration in 0.90 % NaCl (mg l^{-1})	Pre-exposure calculated total metal concentration dosed in NaCl-EBS medium (mg l^{-1})	Measured metal concentration in the supernatant post-bacterial exposure (mg l^{-1}) [b]	Between-replicate percentage coefficient of variation (%)	Nominal test exposure concentration (mg l^{-1})	Pre-exposure calculated total metal concentration dosed in NaCl-EBS medium (mg l^{-1})	Measured metal concentration in the supernatant post-bacterial exposure (mg l^{-1}) [b]	Between-replicate percentage coefficient of variation (%)
$CdCl_2$, CAS 10108-64-2 (Sigma-Aldrich 202908, Lot MKBM1769)	Purity, 99.99 % trace metal basis	3	1.21 Cd	0.477 ± 0.007 Cd	2.6	3	1.21 Cd	0.623 ± 0.005 Cd [d]	1.3
K_2TeO_3, CAS 7790-58-1 (Hopkin and Williams Ltd)	97 % minimum K_2TeO_3	3	1.45 Te	0.049 ± 0.002 Te	8.2	3	1.45 Te	[e]	[e]
CdTe QDs COOH-coated, CAS 1306-25-8 (PlasmaChem GmbH, Lot YF140402) [a]	Diameter, 3 - 5 nm	3	1.11 Cd	0.367 ± 0.009 Cd	4.1	3	1.11 Cd	0.405 ± 0.004 Cd [d]	1.7
			0.18 Te	0.007 ± 0.001 Te	28.3		0.18 Te	0.010 ± 0.0002 Te	2.7
CdTe QDs NH_4^+-coated, CAS 1306-25-8 (PlasmaChem GmbH, Lot YF140402) [a]	Diameter, 3 - 5 nm	3	1.63 Cd	0.142 ± 0.006 Cd	7.0	3	1.63 Cd	0.084 ± 0.009 Cd [d]	18.1
			0.88 Te	0.004 Te [c]	[f]		0.88 Te	0.004 Te [c]	[f]
CdTe QDs PEG-coated, CAS 1306-25-8 (PlasmaChem GmbH, Lot YF140402) [a]	Diameter, 3 - 5 nm	3	1.55 Cd	0.458 ± 0.002 Cd	0.8	3	1.55 Cd	0.468 ± 0.003 Cd [d]	1.0
			0.29 Te	0.014 ± 0.0004 Te	4.5		0.29 Te	0.012 ± 0.0005 Te	7.2

Test material (supplier)	Manufacturer's information [g]	Aerobic growth				Anaerobic growth			
		Nominal test exposure concentration in 0.90 % NaCl (mg l^{-1})	Pre-exposure calculated total metal concentration dosed in NaCl-EBS medium (mg l^{-1})	Measured metal concentration in the supernatant post-bacterial exposure (mg l^{-1}) [b]	Between-replicate percentage coefficient of variation (%)	Nominal test exposure concentration (mg l^{-1})	Pre-exposure calculated total metal concentration dosed in NaCl-EBS medium (mg l^{-1})	Measured metal concentration in the supernatant post-bacterial exposure (mg l^{-1}) [b]	Between-replicate percentage coefficient of variation (%)
$HgCl_2$, CAS 7487-94-7 (Sigma-Aldrich M1136, Lot 071K1201)	Purity, 99 %	3	2.59 Hg	[e]	[e]	3	2.59 Hg	[e]	[e]

[a] Material supplied *via* the NANOSOLUTIONS Project; Quantum dots (QDs); Polyethylene glycol (PEG); Nanoparticles (NPs); Polyvinylpyrrolidinone (PVP);
[b] Data are means ± S.E.M (n = 3 replicates) of total measured metal concentration by inductively coupled plasma optical emission spectrophotometry (ICP-OES) or by inductively coupled plasma mass spectrophotometry (ICP-MS), as appropriate;
[c] Measured value for tellurium below the detection limit of the ICP-MS instrument at 1.122 µg l^{-1};
[d] Indicates a statistical significant difference in measured metal concentration between oxic and anoxic exposure conditions, respectively (t-test, $p < 0.05$);
[e] Not measured;
[f] Not possible to measure;
[g] Brunauer–Emmett–Teller (BET) surface area values (mean ± one standard deviation, n = 3) and zeta potential measurements (mean ± one standard deviation, n = 5) in Milli-Q water, pH 5.0 at 25 ºC using a Zetasizer Nano ZS90 from Malvern Instruments; both provided *via* the NANOSOLUTIONS Project.

887

888 Figure Legends:

889 **Fig. 1** *Escherichia coli* K-12 MG1655 growth, as percentage biomass relative to the normal
890 growth control (no test suspension) and absolute biomass in mg dry weight biomass l^{-1} for: a,
891 b) silver at 3 mg l^{-1} nominal concentration in oxic conditions and 6 mg l^{-1} nominal concentration
892 in anoxic conditions, c, d) copper at 100 mg l^{-1} nominal concentration and, e, f)
893 cadmium/tellurium test materials at 3 mg l^{-1} nominal concentration, unless otherwise stated.
894 Data are mean ± S.E.M (n = 3). Different letters indicate significant differences amongst the
895 relative tested materials (ANOVA, $p < 0.05$) during aerobic and anaerobic growth, respectively.
896 Light shaded grey letters refer to aerobic growth statistical labels and dark grey letters represent
897 anaerobic growth statistical labels. Asterisk (*) refer to significant differences by test material
898 type (t-test, $p < 0.05$) between oxic or anoxic conditions. Complete absence of histogram bars
899 signifies no measurable biomass.

900 **Fig. 2** Absolute growth yield as mean ± S.E.M (g *per* mole of carbon consumed), respectively,
901 where n = 3 from: a) silver at 3 mg l^{-1} nominal concentration in oxic conditions and 6 mg l^{-1}
902 nominal concentration in anoxic conditions, b) copper at 100 mg l^{-1} nominal concentration and,
903 c) cadmium/tellurium at 3 mg l^{-1} nominal concentration, unless otherwise stated. Different
904 letters indicate significant differences amongst the relative tested materials (ANOVA, $p < 0.05$)
905 during aerobic and anaerobic growth, respectively. Light shaded grey letters refer to aerobic
906 growth statistical labels and dark grey letters represent anaerobic growth statistical labels.
907 Asterisk (*) refer to significant differences by test material type (t-test, $p < 0.05$) between oxic
908 or anoxic conditions. Complete absence of histogram bars signifies no measurable yield.

909 **Fig. 3** Measured concentration of fermentation products (mM) as mean ± S.E.M (n = 3): a)
910 acetate, b) ethanol, c) formate, and d) D-, L-lactate, following silver containing test materials
911 exposure relative to the normal growth control (no test suspension) during anaerobic growth of
912 *Escherichia coli* K-12 MG1655. Statistical significant difference amongst the test materials is
913 represented with different letters, where ANOVA, $p < 0.05$. Complete absence of histogram
914 bars signifies no measurable concentration of fermentation product.
915
916 **Fig. 4** Measured concentration of fermentation products (mM) as mean ± S.E.M (n = 3): a)
917 acetate, b) ethanol, c) formate, and d) D-, L-lactate, following copper containing test materials
918 exposure relative to the normal growth control (no test suspension) during anaerobic growth of
919 *Escherichia coli* K-12 MG1655. Statistical significant difference amongst the test materials is

represented with different letters, where ANOVA, $p < 0.05$. Complete absence of histogram bars signifies no measurable concentration of fermentation product.

Fig. 5 Measured concentration of fermentation products (mM) as mean ± S.E.M ($n = 3$): a) acetate, b) ethanol, c) formate, and d) D-, L-lactate, following cadmium/tellurium containing test materials exposure relative to the normal growth control (no test suspension) during anaerobic growth of *Escherichia coli* K-12 MG1655. Statistical significant difference amongst the test materials is represented with different letters, where ANOVA, $p < 0.05$. Complete absence of histogram bars signifies no measurable concentration of fermentation product.

933 **Fig. 1**

934

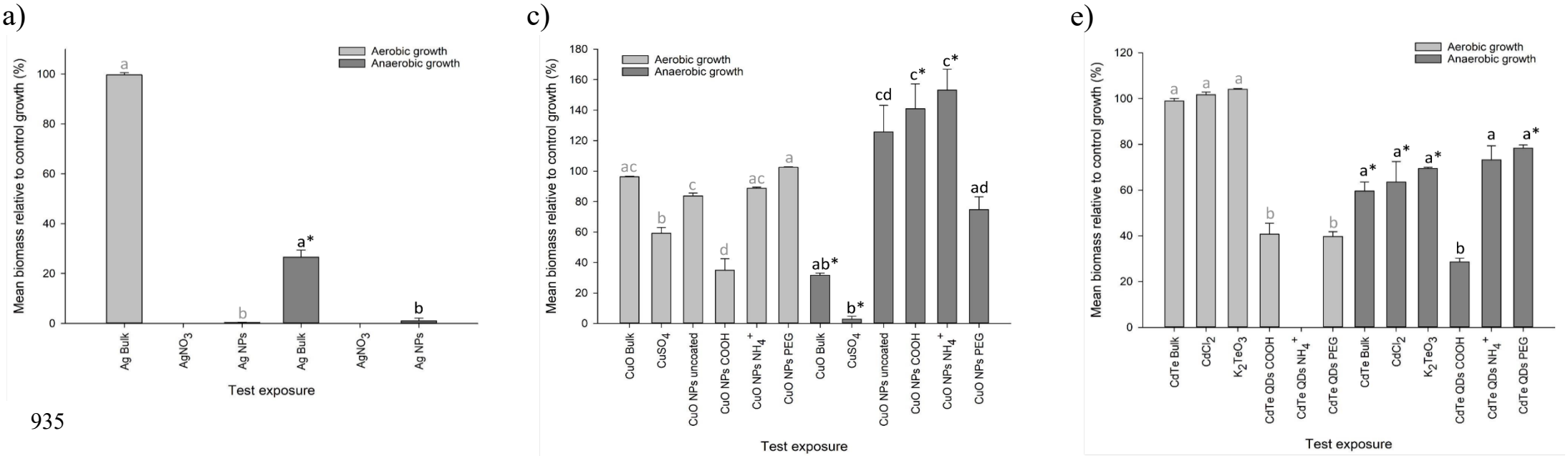

935

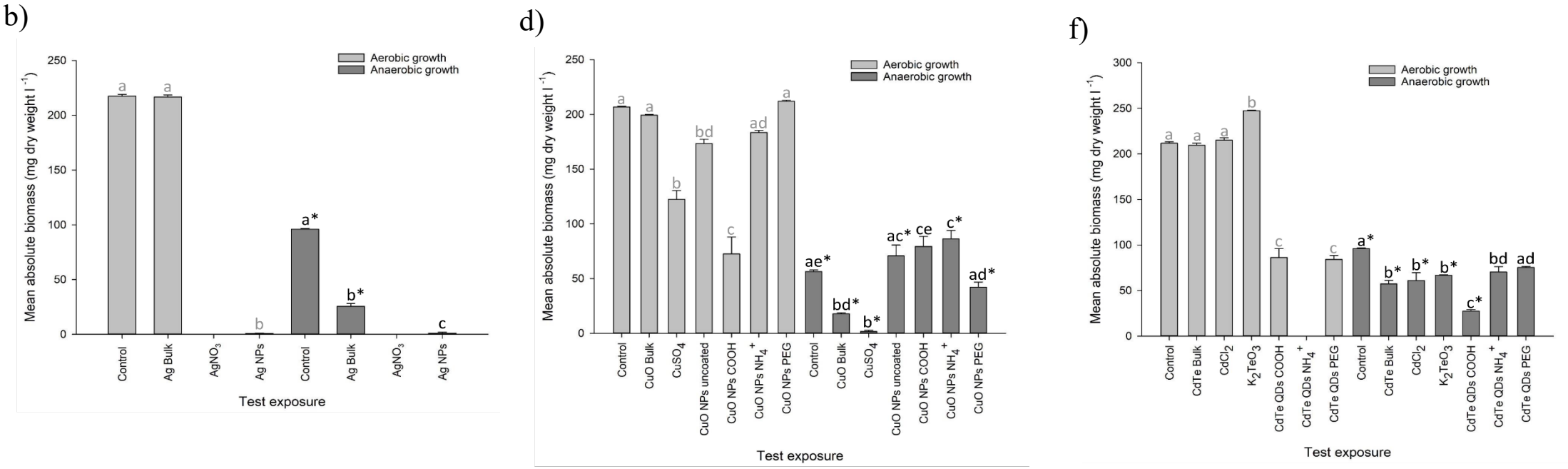

936 **Fig. 2**

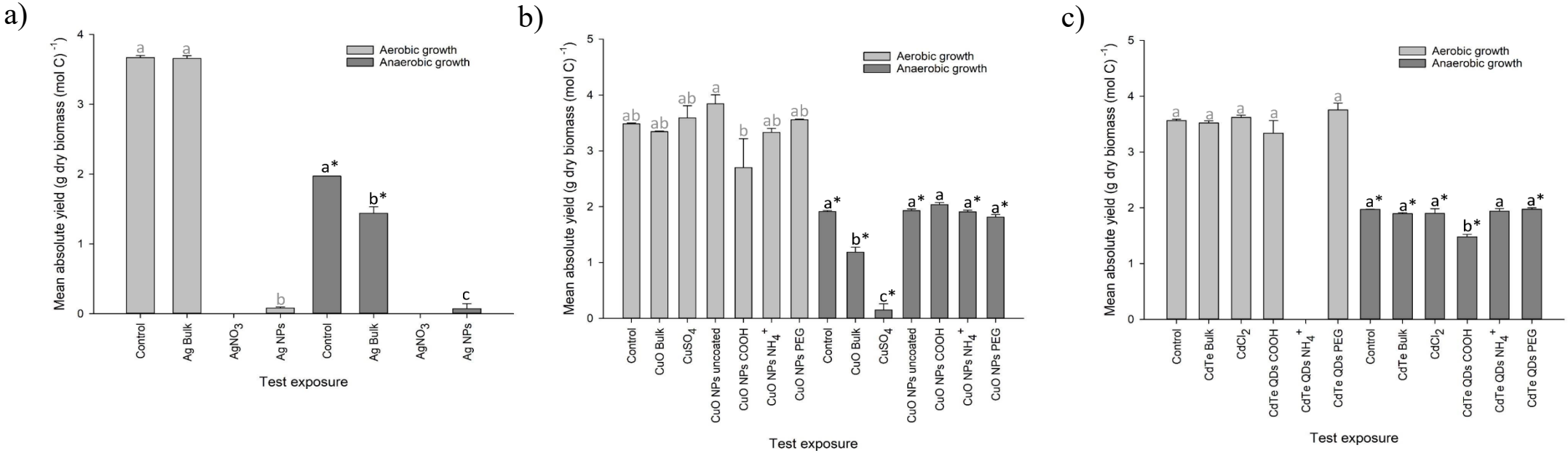
a)
b)
c)
Aerobic growth
Anaerobic growth
Mean absolute yield (g dry biomass (mol C) $^{-1}$)
Test exposure
Control
Ag Bulk
$AgNO_3$
Ag NPs
CuO Bulk
$CuSO_4$
CuO NPs uncoated
CuO NPs COOH
CuO NPs NH_4^+
CuO NPs PEG
CdTe Bulk
$CdCl_2$
CdTe QDs COOH
CdTe QDs NH_4^+
CdTe QDs PEG

937 **Fig. 3**

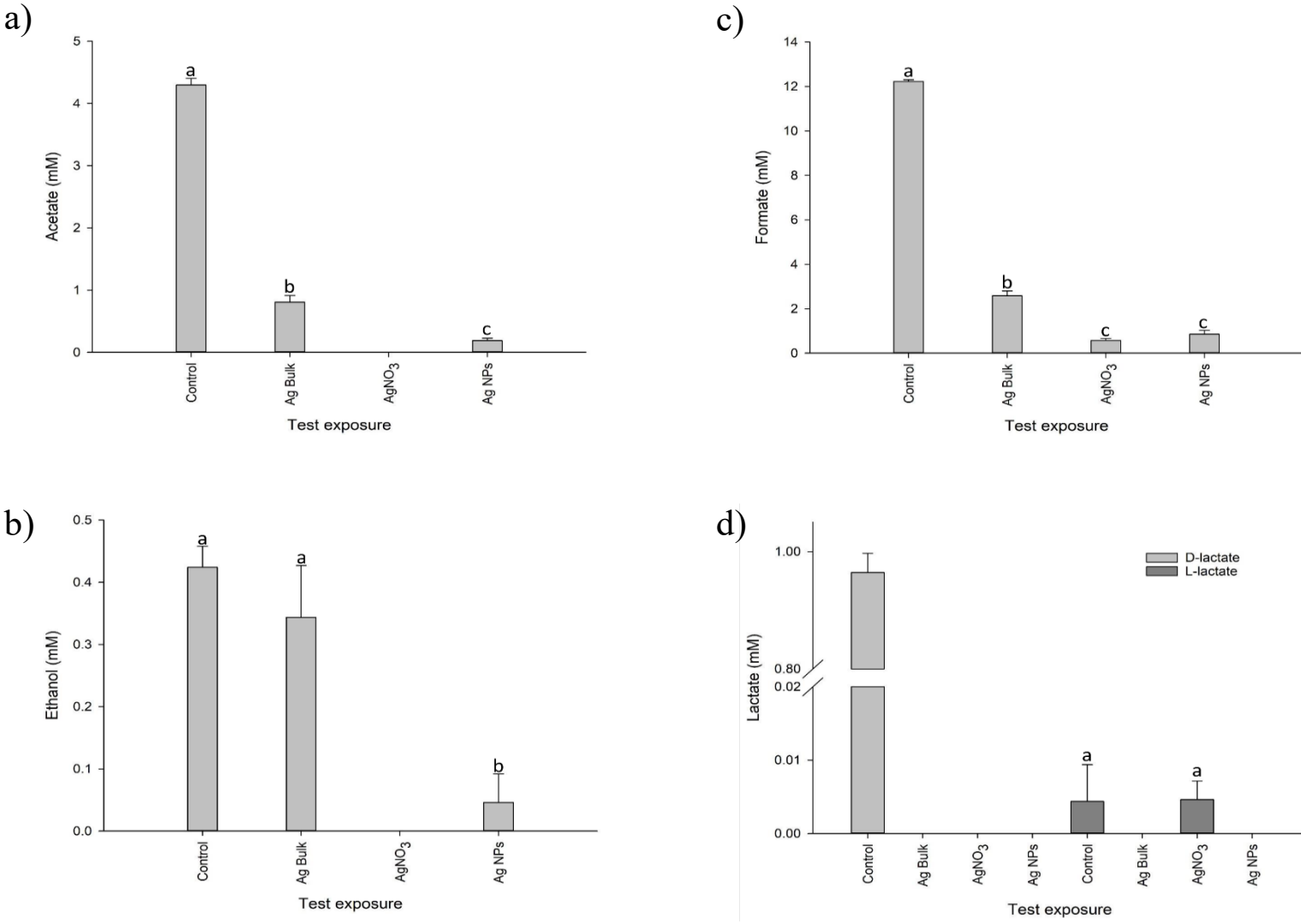

938
939
940
941
942
943
944
945
946
947
948
949
950
951

952 **Fig. 4**

953

a)

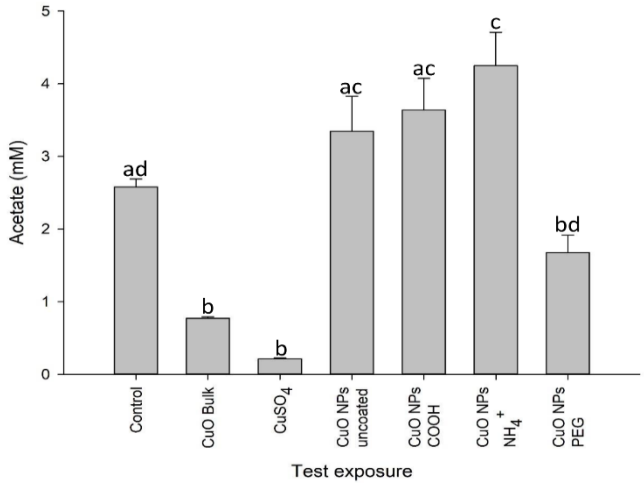

c)

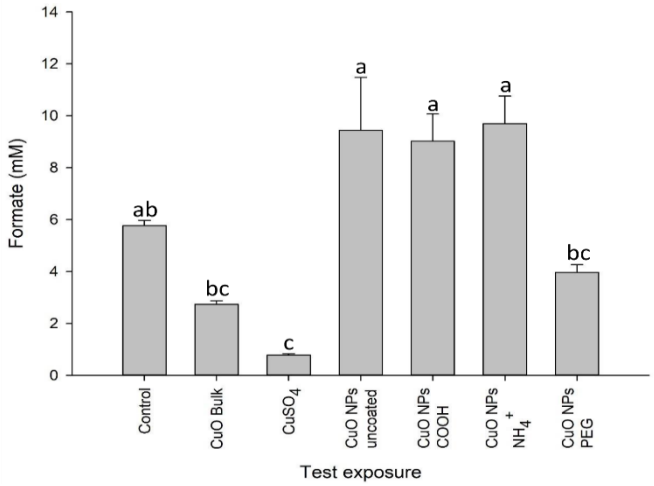

954

b)

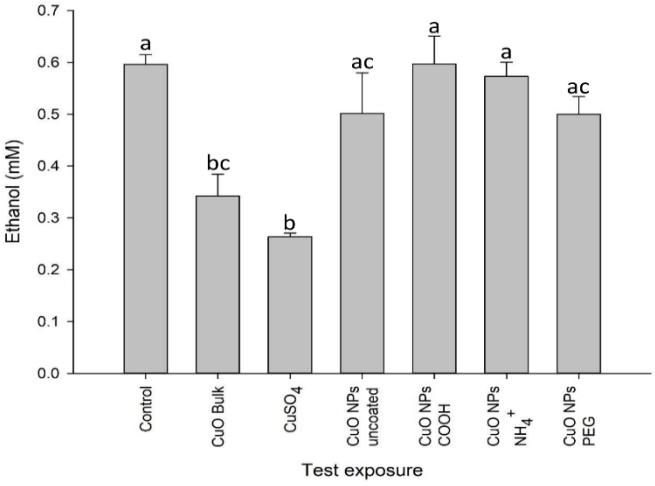

d)

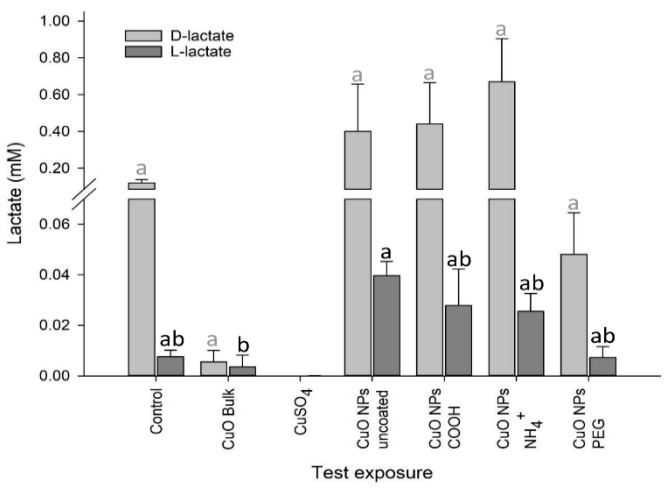

955

956

957

958

959

960

961

962

963

964

965

966 **Fig. 5**
967

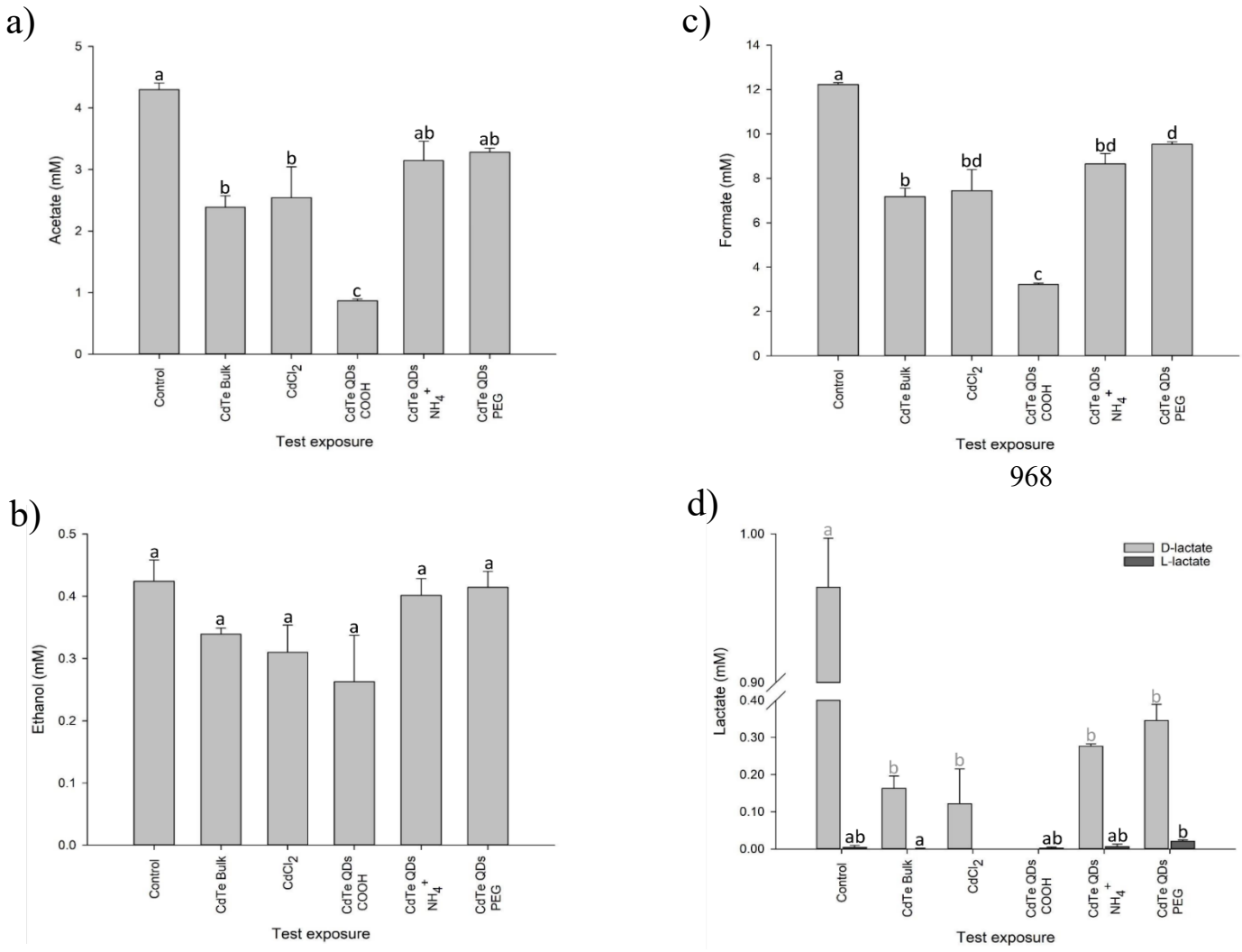

968
969
970
971
972
973